Solid Earth Discuss., 3, 355–383, 2011
www.solid-earth-discuss.net/3/355/2011/
doi:10.5194/sed-3-355-2011

Solid Earth Discussions

New zircon data supporting models of short-lived igneous activity at 1.89 Ga in the western Skellefte District, central Fennoscandian Shield

P. Skyttä[1], T. Hermansson[2], J. Andersson[3], and P. Weihed[1]

[1]Division of Geosciences, Luleå University of Technology, 97187 Luleå, Sweden
[2]Boliden Mineral AB, 93681 Boliden, Sweden
[3]Geological Survey of Sweden, P.O. Box 670, 75128 Uppsala, Sweden

Received: 15 March 2011 – Accepted: 25 March 2011 – Published: 1 April 2011

Correspondence to: P. Skyttä (pietari.skytta@ltu.se)

Published by Copernicus Publications on behalf of the European Geosciences Union.

Abstract

New U-Th-Pb zircon data (SIMS) from three intrusive phases of the Palaeoproterozoic Viterliden intrusion in the western Skellefte District, central Fennoscandian Shield, dates igneous emplacement in a narrow time interval at about 1.89 Ga. A locally occurring quartz-plagioclase porphyritic tonalite, here dated at 1889 ± 3 Ma, is, based on the new age data and field evidence, considered the youngest of the intrusive units. This supports an existing interpretation of its fault-controlled emplacement after intrusion of the dominating hornblende-tonalite units, in this study dated at 1892 ± 3 Ma. The Viterliden magmatism was synchronous with the oldest units of the Jörn type early-orogenic intrusions in the eastern part of the district (1.89–1.88 Ga; cf. Gonzàles Roldán, 2010). A U-Pb zircon age for a felsic metavolcanic rock from the hanging-wall to the Kristineberg VMS deposit, immediately south of the Viterliden intrusion, is in this study constrained in the 1.89–1.88 Ga time interval. It provides a minimum age for the Kristineberg ore deposit and suggests contemporaneous igneous/volcanic activity throughout the Skellefte District. Furthermore, it supports the view that the Skellefte Group defines a laterally continuous belt throughout this "ore district". Tentative correlation of the 1889 ± 3 Ma quartz-plagioclase porphyritic tonalite with the Kristineberg "mine porphyry", which cuts the altered ore-hosting metavolcanic rocks, further constrain the minimum age for ore deposition at 1889 ± 3 Ma. Based on the new age determinations, the Viterliden intrusion may equally well have intruded into, or locally acted as a basement for the ore-hosting Skellefte Group volcanic rocks.

1 Introduction

The Skellefte District (Fig. 1) is one of the most important mining districts in northern Europe with numerous VMS deposits and a large potential for future discoveries (Carranza and Sadeghi, 2010). The Kristineberg mine is located in the western part of the district. It is the largest past and present VMS mine in the district, with a total production of 26.5 Mt ore, grading 1.05 Cu %, 3.56 Zn %, 0.24 Pb %, 1.31 $g\,t^{-1}$ Au, 38 $g\,t^{-1}$ Ag, and 25.6% S, from the start of production in 1940 to the end of year 2010. The deposit is hosted by felsic to intermediate metavolcanic rocks suggested to be part of the ore hosting, 1.89–1.88 Ga Skellefte Group that occurs throughout the Skellefte District (cf. Allen et al., 1996; Kathol and Weihed, 2005). The ore-hosting metavolcanic rocks structurally overlie the composite, pre-tectonic ~1.90 Ga Viterliden intrusion (Bergström et al., 1999; Skyttä et al., 2010), both occurring in the core of a regional-scale antiformal structure (Fig. 1; Skyttä et al., 2009). Previous geochronological work in the Skellefte District has been focused on the metavolcanic and granitoid rocks of the eastern and central parts (Billström and Weihed, 1996; Lundström and Antal, 2000; Weihed et al., 2002; Gonzàles Roldán, 2010). Apart from the composite Viterliden intrusion dated at 1907 ± 13 Ma by Bergström et al. (1999), age data from the western part of the Skellefte District is lacking and the time scale of volcanic activity is unknown. Correlation of the Kristineberg volcanic and intrusive units in the west with the ore-bearing Skellefte Group volcanic, and early-orogenic calc-alkaline intrusive units in the other parts of the Skellefte District, requires control over the timing of magmatism across the district. Furthermore, temporal relationships between intrusive and volcanic events are needed to indirectly constrain the age of the VMS mineralization, and to better understand the crustal-scale accretionary processes during the Svecokarelian orogeny.

This study presents new U-Th-Pb zircon data from four different igneous units in the Kristineberg area in the western part of the Skellefte District: three compositionally different intrusive units of the composite Viterliden intrusion and one volcanic unit within the stratigraphic hanging-wall to the Kristineberg deposit. Besides constraining the emplacement history of the composite intrusion, dating several intrusive units from a geographically small area aims at investigating the consistency of igneous zircon crystallization ages within different magmatic components of this plutonic complex. The latter is especially important because of the relatively old published age of the Viterliden intrusion with respect to the other early-orogenic intrusive units in the district (Wilson et al., 1987; Weihed and Schöberg, 1991; Lundström et al., 1997; Bergström et al., 1999; Weihed et al., 2002; Gonzàles Roldán, 2010). Dating the metavolcanic rock aims at correlating the volcanic units in different parts of the Skellefte District, and at providing an estimate for the minimum age of the mineralization of the Kristineberg deposit. The obtained age data will be interpreted and discussed with respect to the evolution of igneous activity in the Skellefte District, with special emphasis on the timing of VMS mineralization at Kristineberg.

2 Geological overview

2.1 Geological and structural setting

The bedrock of the Skellefte District is composed of 1.95–1.85 Ga Palaeoproterozoic Svecofennian supracrustal and associated intrusive rocks that were deformed and metamorphosed during the Svecokarelian orogeny at 1.87–1.80 Ga (Weihed et al., 2002). The majority of models for the crustal evolution of the Skellefte District suggest that it is a remnant of a volcanic arc accreted towards the Karelian craton in the NE (Hietanen, 1975; Gaál, 1990; Weihed et al., 1992). However, an alternative interpretation has been presented by Rutland et al. (2001a, b) and Skiöld and Rutland (2006), who suggest that the Skellefte District was deposited in a rift setting on the Bothnian Basin metasedimentary rocks (their Robertsfors Group) during an episode of crustal extension related to a contemporaneous active margin located west of the present exposure of Svecofennian rocks. 2.0–1.9 Ga granitoids south of the Skellefte district (Billström and Weihed, 1996) and the Bothnian Basin rocks beneath a N-dipping crustal-scale reflector in the Kristineberg area (Malehmir et al., 2007) have also been suggested to be the basement of the Skellefte District. The contacts of the Skellefte District and the Arvidsjaur Group volcanic rocks in the north, and the Bothinan Basin metasedimentary rocks in the south are not exposed.

SED
3, 355–383, 2011

The structural evolution of the Skellefte District is controlled by a complex fault pattern developed during early crustal extension (Allen et al., 1996; Bauer et al., 2011). The early normal and related transfer faults were later inverted during crustal shortening (Bauer et al., 2009; Skyttä et al., 2010). The main compression in the Skellefte District was related to ~N-S shortening, which led to dominantly reverse S-block-up faulting, and development of related upright folds with curvilinear fold axes in the central part of the district (Bergman Weihed, 2001; Bauer et al., 2011). In the Kristineberg area, a regional-scale antiform with a variably W-plunging hinge was formed during to the same deformation phase. A maximum age for this event is constrained at ~1.87 Ga by the youngest rock unit it deformed, namely the 1875±4 Ma Vargfors Group (Billström and Weihed, 1996; Bergman Weihed, 2001). Intrusion of the late-orogenic granitoids at ≤1.82 Ga constrain the minimum age of this event at ~1.82 Ga (Weihed et al., 2002), and cross-cutting relationships between granitoid dykes, deformation fabrics and folding events (Rutland et al., 2001b), and ID-TIMS analyses of monazites southwest from the Skellefte District (Skiöld and Rutland, 2006) tighten the constraints even further to ~1.88–1.85 Ga. Another episode of crustal shortening took place at ~1.80 Ga, and was characterized by ~E-W bulk compression which resulted in reverse faulting along major ~N-S trending shear zones in the central Skellefte District and dextral strike-slip reactivation of the early reverse faults in the Kristineberg area (Bergman Weihed, 2001; Weihed et al., 2002; Skyttä et al., 2010). Metamorphic peak conditions reached partial melting in the south-eastern part of the district, whereas sub-solidus PT-conditions at ~3 kbars and ~600 °C prevailed in the Kristineberg area at ~1.85–1.80 Ga (cf. Kathol and Weihed, 2005).

2.2 Lithology

The Skellefte District comprises three main groups of supracrustal rocks and four generations of intrusive rocks (Weihed et al., 2002 and references therein). The supracrustal rocks include the predominantly metavolcanic Skellefte and Arvidsjaur Groups, and the predominantly metasedimentary Vargfors Group. The

SED
3, 355–383, 2011

New zircon data supporting models of short-lived igneous activity at 1.89 Ga

P. Skyttä et al.

intrusive generations consist of (Fig. 1): (1) pre-1.88 Ga, early-orogenic, calc-alkaline granodiorites-tonalites and gabbros ("Jörn-type"), (2) 1.88–1.87 Ga alkaline granites-syenites-monzonites (Gallejaur-Arvidsjaur or Perthite-monzonite-suite), (3) 1.82–1.80 Ga minimum melt S-type granites (Skellefte- and Härnö-type), and (4) 1.80–1.78 Ga coarse-porphyritic, A- to I-type granites, monzonites and diorites (Revsund type). The Bothnian Basin metasedimentary rocks occur within a large area south of the Skellefte District, and have been suggested to make up the basement for the Skellefte Group rocks (Skiöld and Rutland, 2006). However, the prolonged sedimentation lasting from pre- to post-Skellefte Group (>1.95 Ga to 1.87 Ga; Weihed et al., 2002 and references therein), leaves their stratigraphic position partly open.

The predominantly felsic, volcanic Skellefte Group is attributed to a stage of extensional continental margin arc volcanism (Allen et al., 1996), and constitutes the lowermost supracrustal unit in the Skellefte District stratigraphy (Figs. 2 and 3). It is the main host to the VMS deposits, the majority of which are located within the upper part of the unit (Allen et al., 1996). Age of the Skellefte Group volcanism has been dated at ~1.89–1.88 Ga by U-Pb data on zircons from the central part of the Skellefte District (Welin, 1987; Billström and Weihed, 1996). The Vargfors Group lies stratigraphically above the Skellefte Group rocks, and is characterized by turbidites, sandstones and conglomerates. A 1875 ± 4 Ma ignimbrite intercalated with the Vargfors Group metasedimentary rocks (Billström and Weihed, 1996) implies that they were coeval with deposition of the sub-aerial Arvidsjaur Group occurring further to the north (Skiöld et al., 1993).

The Jörn-type calc-alkaline intrusives (Fig. 1; Björkdal, Jörn, Siksträsk, Karsträsk, Rengård and Viterliden intrusions) range between ~1.91 and 1.86 Ga in age, thus forming the oldest group of intrusives in the Skellefte District and its immediate surroundings. The tonalitic Sikträsk intrusion (1878 ± 12 Ma; Weihed et al., 2002) and the oldest GI phase of the Jörn intrusive complex (1.89–1.88 Ga; Wilson et al., 1987; Weihed and Schöberg, 1991; Lundström et al., 1997; Gonzàles Roldán, 2010) are coeval with the Skellefte Group volcanism, and considered co-magmatic, whereas the younger phases of the complex (GII-III; 1.88–1.86 Ga; Wilson et al., 1987; Weihed and Schöberg, 1991; Lundström et al., 1997; Gonzàles Roldán, 2010) post-date the Skellefte Group. Even though the Viterliden intrusion at Kristineberg (1907 ± 13 Ma; Bergström et al., 1999) is supposed to be older than most of the other intrusions, its marginal phase, the "mine-porphyry", contains xenoliths of altered Skellefte Group metavolcanic rocks and, consequently, post-dates the ore-related alteration (Årebäck et al., 2005). The Gallejaur intrusion consists of a felsic core mingling with a mafic rim, dated at 1873 ± 10 Ma and 1876 ± 4 Ma, respectively (Skiöld, 1988; Skiöld et al., 1993), and is contemporaneous with the Gallejaur mafic lavas intercalated with the Vargfors Group metasedimentary rocks (Kathol and Weihed, 2005). Late- to post-Svecokarelian 1.82–1.78 Ga intrusive rocks occur to the west and south of the Kristineberg antiform (Weihed et al., 2002 and references therein).

2.3 The Viterliden intrusion and the Kristineberg hanging-wall rhyolite

The Viterliden intrusion and the Kristineberg VMS deposit occur in the core of the Kristineberg antiform, which is considered to be a result of early extension (Allen et al., 1996; Bauer et al., 2011) overprinted by crustal shortening, characterised by inversion of the normal faults under ~N-S compression (Fig. 3; Skyttä et al., 2010). The greatest strains were localised into these sub-vertical, curviplanar faults and their vicinities, which led to large variations in strain and structural geometry both across and along the regional antiformal structure (Malehmir et al., 2007, 2009; Skyttä et al., 2009; Dehghannejad, 2010). Intense mylonitic fabrics developed in the high-strain zones, whereas weak to moderate foliation characterizes the low-strain lenses in-between. The foliation in the low-strain areas is penetrative and mostly defined by alignment of mica grains, whereas hornblende grains occur both as elongated grains sub-parallel to the mica, and as more equant grains or aggregates showing no distinct preferred orientation, defining a SL-shape fabric. Within the high-strain zones, but also locally within the tectonic lenses, the rocks are dominantly LS- to L-tectonites (e.g. at locality I; Fig. 2). Mineral lineation is defined by the zonal orientation of mica and the alignment of hornblende. In high-strain zones, it plunges either down-dip when associated with

SED
3, 355–383, 2011

reverse dip-slip kinematics, or sub-horizontally when associated with dextral strike-slip kinematics.

The Viterliden meta-intrusion comprises hornblende-tonalites (Fig. 4a), plagioclase porphyritic tonalites (Fig. 4b), granites, quartz-plagioclase porphyritic tonalites (Fig. 4d and e; "mine porphyry" by Årebäck et al., 2005). It also hosts high-strain zones characterized by boudinaged intrusives embedded in a mica-rich, mylonitic matrix. The hornblende-tonalites are medium- and even-grained, and are composed of quartz (qtz), plagioclase (plg), hornblende (hbl), biotite (bt), magnetite (mt), pyrite (py) and sphalerite (sph) (± chlorite (chl), ± titanite (tita); totally ~30% mafic minerals). Plagioclase porphyritic tonalites are characterized by large plg-megacrysts surrounded by finer-grained matrix composed of qtz, plg, bt (± muscovite (ms); totally ~15% mafic minerals). Granites display qtz-plg-kfs rich domains separated by thinner, discontinuous domains of bt, ms, and chl (totally ~10% mafic minerals), which gives the rock a streaky appearance. Opaque minerals include mt, py and chalcopyrite (cpy). Quartz-plagioclase porphyritic tonalites contain phenocrysts of qtz and plg in a finer-grained matrix composed of qtz, feldspars (fsp), ms, bt and chl (totally ~10% mica content). The matrix grain size in the southern quartz-plagioclase porphyritic tonalite is significantly larger compared to the "mine porphyry" in the north.

The hornblende-tonalites are volumetrically dominating, whereas the other lithologies are clearly subordinate, in particular the quartz-plagioclase porphyritic tonalites that are associated with E-W to NE-SW trending fault zones only (Fig. 2). Contacts between the different intrusive phases, as well as contacts between the intrusion and the bounding volcanic rocks are generally sheared. For this reason, initial relative age relationships are inaccessible. The Kristineberg hanging-wall rhyolite (Fig. 4c) is fine-grained, contains up to 0.2 mm large qtz- and plg-phenocrysts in a fine-grained matrix of qtz, fsp and bt (totally <10% mafic minerals), and have a well developed a SW-plunging lineation defined by elongate bt-aggregates. The hanging-wall rhyolite is associated with the stratigraphically lower of the two ore horizons in the Kristineberg area, the Kristineberg-Kimheden ore horizon (Figs. 2, 3). The

SED
3, 355–383, 2011

stratigraphically higher, Hornträsk-Rävlidsmyran-Rävliden ore horizon is located in the upper part of the Skellefte Group volcanic rocks, which is the most common stratigraphic position for VMS deposits in the Skellefte District. Based on alteration patterns, the mine porphyry vs. the ore-hosting metavolcanic rock cross-cutting relationship, and geochemical modelling, Galley and Bailes (unpublished data, 1999) suggested that the development of the lower of the Kristineberg ore horizons was associated with a pre-Viterliden subvolcanic intrusion at depth. In contrast, the upper ore horizon was considered coeval with the emplacement of the Viterliden intrusion into the volcanic pile (Galley and Bailes, unpublished data, 1999).

3 Geochronology

3.1 Sampling and analytical procedures

A total of seven samples were selected for geochronological analyses from the Kristineberg area. The samples were taken both at the surface and from drill cores available in the Boliden Mineral AB drill core archives. They were milled into fine-grained powder using a swing-mill. Heavy mineral separates were obtained using a full size Wilfley water panning table. Magnetic mineral fractions were removed with a hand-magnet. Zircon grains selected for further analytic work were hand-picked using a stereomicroscope. Since all samples are rather poor in zircon, as much as about 10 kg of rock were processed for most samples. Of all seven samples, zircon was only recovered in three meta-intrusive and one metavolcanic rock.

Zircons selected for analytical work were mounted on double-faced tape and embedded in transparent epoxy resin together with the 1065 Ma Geostandards zircon 91 500 (Wiedenbeck et al., 1995). The epoxy mount was polished to expose the central parts of the crystals, including the potentially older cores.

Back scattered electron (BSE) imaging was used for selection of the location of analytical spots and subsequent re-examination of spot sites after analysis. The

SED
3, 355–383, 2011

BSE-imaging prior to analysis was done at the Luleå University of Technology in Luleå using a Phillips XL30 electron microscope with LaB6 filament. Post-analysis BSE-imaging was done at the Evolutionary Biology Centre at Uppsala University using a Zeiss Supra 35-VP field emission SEM electron microscope, with a Robinson back scatter detector. Prior to U-Th-Pb analysis, the mount was coated with ca. 30 nm of gold. Secondary Ionisation Mass Spectrometry (SIMS) U-Th-Pb in situ analyses on zircon was carried out using a Cameca IMS 1280 high mass-resolution instrument, at the NORDSIM facility at the Swedish Museum of Natural History in Stockholm. The analytical procedures followed Whitehouse et al. (1999) and Whitehouse and Kamber (2005). The instrument was operated with a spot size less than 25 µm.

All isotopic data are presented in Table 1. Age calculations were done using Isoplot/Ex (Ludwig, 2003). Ages are reported with 2 sigma errors, except for sample 60.1-pmsk-09, which is reported with 95%-confidence limits. In the figures, and in the discussion, concordia ages are presented without decay constant errors. However, in the section below, age calculations are presented both with and without decay constant errors, for future reference.

3.2 Sample descriptions and U-Pb results

3.2.1 Sample I: Viterliden hornblende-tonalite (47.1-pmsk-09)

Zircon was quite abundant in the sample that is dominated by up to 0.6 mm long, euhedral prismatic grains with sharp terminations. The crystals have approximate width/length ratios of 1:3, and are transparent to semi-transparent and colourless to weakly yellowish (light brownish) in colour. Most grains are cracked. The sample also contains a subordinate group of small (up to 150 µm), rounded and slightly brownish grains. In BSE-images, the zircons typically show broad-banded, simple oscillatory zoning without texturally complex core-rim relationships (Fig. 5, n3448-01ab). Consequently, both the external morphology and the internal textures suggest a well-preserved igneous character of the zircon in this sample (cf. Corfu et al., 2003).

SED
3, 355–383, 2011

A total of fifteen analyses were obtained in thirteen different crystals. Two analyses are more than 5% discordant (n3448-06b and 13a). Both hit cracks and were excluded from age calculation. The remaining thirteen concordant analyses yield a concordia age (ignoring decay constant errors) of 1892 ± 3 Ma (Fig. 6a; $MSWD_{conc.+equiv.}$ = 1.2, probability = 0.24) identical to the weighted average $^{207}Pb/^{206}Pb$ age of 1891 ± 3 Ma (MSWD = 0.86, probability = 0.59).The concordia age including decay constant errors is 1894 ± 5 Ma ($MSWD_{conc.+equiv.}$ = 1.14, probability = 0.28). The well-preserved igneous appearance of the zircon population and the limited spread in the U-Th-Pb data suggests negligible post-igneous crystallisation isotopic disturbance. The concordia age of 1892 ± 3 Ma is interpreted to date igneous crystallisation of the hornblende tonalite.

3.2.2 Sample II: Viterliden plagioclase porphyritic tonalite (33.1-pmsk-08)

Processing of the sample gave a moderate yield of zircon. The analytical quality of the population is rather poor and cracks and inclusions (both dark and colourless) are frequent. The crystals are typically subhedral prisms, with rounded outer terminations. They are between 100–200 µm long with aspect ratios of about 1:2. Uncracked domains are clear to semi-transparent, often with a yellow/orange tint. In BSE-images the zircons generally show a weak broad-banded oscillatory zoning, whereas some marginal domains appear more or less unzoned (Fig. 5, n3450-03ab). Some grains display intense oscillatory zoning in specific domains, which are typically cracked and appear more altered (Fig. 5, n3450-21a). Most grains are texturally non-complex. However, some grains contain texturally older core domains, surrounded and cut by texturally younger unzoned or weakly oscillatory zoned zircon (Fig. 5, n3450-05a, 12a). Secondary alteration features in the zircon population typically occur as BSE-dark thin alteration fronts preferentially located along the outer margins of the grains broadly following bands in the zoning of the crystal. These domains are interpreted as poorly crystalline regions, tentatively indicating progressive metamictisation of the grain.

SED
3, 355–383, 2011

The low analytical quality of the zircon population made it difficult to locate areas devoid of cracks, inclusions, and BSE-dark altered domains large enough to host an analytical spot. As a consequence, 18 of the totally 32 analytical spots hit cracks, inclusions or straddled the crystal margin-epoxy interface. This resulted in a varying degree of discordance for these analyses (Table 1), which show a more or less complex pattern indicating both ancient and recent Pb-loss. The discordant data were excluded from the age calculation. The remaining 14 concordant analyses were located in domains showing a weak, broad banded BSE-zoning, covering both internal and marginal parts of the crystals. Together the 14 concordant analyses define a concordia age (ignoring decay constant errors) of 1891 ± 3 Ma (Fig. 6b; $\mathrm{MSWD}_{\mathrm{conc.+equiv.}} = 1.4$, probability = 0.082), identical to a weighted average $^{207}\mathrm{Pb}/^{206}\mathrm{Pb}$ age of the same analyses at 1892 ± 4 Ma (MSWD = 0.89, probability = 0.56). The concordia age including decay constant errors is 1890 ± 5 Ma ($\mathrm{MSWD}_{\mathrm{conc.+equiv.}} = 1.4$, probability = 0.086). The 1891 ± 3 Ma concordia age is interpreted to directly date igneous crystallisation of the plagioclase porphyritic tonalite.

3.2.3 Sample III: Viterliden quartz-plagioclase porphyritic tonalite (coarse "mine porphyry"; 29.1-pmsk-08)

The zircon population is dominated by prismatic, typically between 100–250 µm long, and more or less euhedral crystals with length/width ratios of 2.5–3. They are semi-transparent light-brown to nearly colourless, with slight orange shades. Cracks and inclusions are common. In BSE-imaging, the crystals typically show an intense, but somewhat blurred oscillatory zoning that in most grains continues throughout the grain all the way to the crystal edge (Fig. 5, n3449-02a, 03a). This is indicative of a single non-complex growth stage.

A total of 27 analyses were made in 25 different crystals. The analytical result is affected by the abundance of cracks and inclusions in the analysed zircon population. 18 out of 27 analyses are between 1–46% discordant. This discordance is directly correlated to the location of the analytical spot hitting cracks or inclusions, or the crystal-epoxy interface (see location of analysed area in Table 1). U contents in un-cracked, inclusion-free domains are between 350–660 ppm. Discordant analyses, where the analytical spot has hit cracks and/or inclusions, may have up to 1000 ppm U and generally also significantly higher amounts of common Pb ($^{206}Pb/^{204}Pb$ ratios often well below 10 000, Table 1). These analyses have been excluded from the age calculation. The remaining nine analyses are concordant and give a concordia age (ignoring the decay constant errors) of 1889 ± 3 Ma (Fig. 6c; $MSWD_{conc.+equiv.} = 1.4$, probability = 0.13), identical to a weighted average $^{207}Pb/^{206}Pb$ age of the same analyses calculated at 1890 ± 4 Ma (MSWD = 1.1, probability = 0.33). The concordia age including decay constant errors is 1888 ± 6 Ma ($MSWD_{conc.+equiv.} = 1.4$, probability = 0.14). The concordia age defined by the nine concordant analyses is interpreted to date igneous crystallisation of the quartz-plagioclase porphyritic tonalite at 1889 ± 3 Ma.

3.2.4 Sample IV: Kristineberg hanging-wall rhyolite (60.1-pmsk-09)

About 50 zircons were retrieved from a 10 kg sample of the Kristineberg hanging-wall rhyolite. The crystals are rather small in size, typically short prismatic and more or less euhedral with aspect ratios between 1:2 and 1:3, and maximum lengths of about 150 µm. They are turbid and semi-transparent and cracks and inclusions are common. In BSE-images the zircons are texturally uniform, typically showing a weak broad-banded zoning or are unzoned (Fig. 5, n3447-32b, 22a). The textures suggest a non-complex single stage of zircon growth.

A total of 37 analyses were obtained from the sample. 24 of these are discordant and several of these significantly reversely discordant (Fig. 6d). In contrast to the other three samples, there is no obvious correlation between discordance and location of analytical spot at inclusions, cracks or at across the crystal-epoxy interface. Furthermore, the concordant data points spread too much in age to define a common concordia age. The analyses on this sample were acquired in the same analytical sub-session as

SED
3, 355–383, 2011

the other samples, in which the analytical conditions, the standard calibration, and the obtained data are of high quality. The rhyolite zircons are located in an area relatively close (5 mm) to the margin of the epoxy mount. The sample-dependent analytical problems observed for the Kristineberg rhyolite zircon data, might be caused by analytical disturbance arising from the location of the sample in the sample holder, and not by geological processes.

13 of the 37 analyses are concordant within 2 sigma errors (Table 1). Three of these analyses were discarded from the age calculation. Two of them, since their error ellipses do not cross-cut the concordia line (n3447-10a and 19a), and one because the analysis gives distinctly deviating isotopic ratios, with large errors (n3447-31a). The remaining ten concordant analyses define a concordia age (ignoring decay constant errors) of 1886 ± 9 Ma ($MSWD_{conc.+equiv.} = 2.0$, probability = 0.007) and a weighted average $^{207}Pb/^{206}Pb$ age of the same ten analyses calculated at 1883 ± 7 Ma (MSWD = 1.12, probability = 0.35). The concordia age including decay constant errors is 1888 ± 10 Ma ($MSWD_{conc.+equiv.} = 1.9$, probability = 0.009). The igneous crystallisation of the Kristineberg Rhyolite is here dated at between 1.89–1.88 Ga. Calculation of a more precise age is hampered by sample-specific analytical problems described above.

4 Discussion

The new ∼1.89 Ga U-Pb ages for the three different phases of the composite Viterliden intrusion demonstrate that it was emplaced synchronously with the majority of the pre- to early-orogenic granitoids further east in the Skellefte District (Wilson et al., 1987; Weihed and Schöberg, 1991; Lundström et al., 1997; Weihed et al., 2002; Gonzàles Roldán, 2010). Exceptions are the ∼1.91 Ma Björkdal intrusion (Lundström and Antal, 2000) and the younger phases of the Jörn intrusive complex (Gonzàles Roldán, 2010). Of these two, the Björkdal intrusion has a complex history including several zircon-forming events (Lundström and Antal, 2000), and for this reason, it is not clear if it may

SED
3, 355–383, 2011

be classified into the group of Jörn type intrusives. According to recent petrological investigations of the younger phases of the Jörn intrusive complex (GIII-IV; 1.87 Ga) it is not likely that they are cogenetic with the older 1.89–1.88 Ga GI-phase (Gonzàles Roldán, 2010). The 1.89–1.88 Ga age for the Kristineberg hanging-wall rhyolite shows that not only intrusive, but also felsic volcanic activity was synchronous throughout the whole Skellefte District, culminating at ~1.89 Ga (cf. Welin, 1987; Billström and Weihed, 1996). This also supports the idea that the Skellefte District was originally a laterally (sub)continuous volcanic belt (Carranza and Sadeghi, 2010), that was later split and transposed by tectonic events (Skyttä et al., 2010). The new geochronology data presented here, highlight the importance of the 1.89 Ga igneous activity in the build-up of the Skellefte District. The synchronous timing of the igneous events allows for geological correlations throughout the Skellefte District.

The relationship between the intrusive and volcanic units in the Skellefte District is important, since it affects interpretations on the mineralization processes. Because nearly all early-orogenic intrusions within the district (e.g. Karsträsk, Sikträsk, Rengård; Fig. 1) experienced high degrees of tectonic transposition, often including development of shear zones along their margins (Bergman Weihed et al., 2001), it is not possible with the available data to constrain their stratigraphic position relative to the surrounding metavolcanic rocks. Not even from the now reasonably well-dated Kristineberg area is it possible to satisfactorily determine the temporal relationship between all the intrusive phases and the structurally overlying volcanic sequence. The regionally overlapping ages of the early-orogenic intrusives (Wilson et al., 1987; Weihed and Schönberg, 1991; Lundström et al., 1997; Weihed et al., 2002; Gonzàles Roldán, 2010) and the Skellefte Group metavolcanic rocks (Welin, 1987; Billström and Weihed, 1996) are in agreement with the idea that the Viterliden complex intruded into the succession of Skellefte Group metavolcanic rocks (Galley and Bailes, unpublished data, 1999). This is also supported by the xenoliths of altered ore-hosting metavolcanic rocks in the "mine porphyry" at Kristineberg (Årebäck et al., 2005). The new data presented here, show that the volumetrically largest phases of the Viterliden intrusion probably are slightly older than the Kristineberg hanging-wall rhyolite. For this reason, it is possible that these parts of the intrusive complex acted as a basement for the overlying volcanic rocks. This interpretation agrees with Billström and Weihed (1996), who considered the Sm-Nd signature of the Skellefte Group metavolcanic rocks to indicate the presence of an intrusive basement, not much older than the metavolcanic rocks themselves. However, the new data does not exclude the possibility that the whole complex is intrusive into the volcanic sequence, since it only constrains the relationship between the intrusion and the hanging-wall rhyolite. The age of the volcanic footwall rocks still remains unknown. Furthermore, the interpretation, which considers part of the intrusive complex to be the basement to the volcanic sequence, would require some time for erosion and uplift between the crystallisation of the intrusion and the onset of volcanism. This may have been accomplished by normal faulting-related footwall uplift prior to, or in the early stages of extension-related volcanism. Regionally, pre-compressional uplift and unroofing of the Jörn GI-type granitoids are attributed to major dip-slip faulting along the intrusive-volcanic contact in the central part of the Skellefte District (Bauer, 2010). However, uplift-related granitoid clast-conglomerates, similar to those in the central Skellefte District area, are lacking in the Kristineberg area.

The "mine porphyry" is considered the youngest of the Viterliden intrusive phases (Galley and Bailes, unpublished data, 1999; Årebäck et al., 2005), but no geochronological evidence has been provided. The overlapping or perhaps slightly younger age of the qtz-plg-porphyritic tonalite presented in this paper (1889 ± 3 Ma), with respect to the other tonalite types (1892 ± 3 Ma; 1891 ± 3 Ma), may support this interpretation. Such a relative timing is also supported by Skyttä et al. (2010), who proposed that the qtz-plg-porphyritic tonalites were emplaced along fault zones truncating the hornblende-tonalites. However, since no zircon was obtained from the "mine porphyry proper" the possibility still remains that it is even younger than the 1889 ± 3 Ma age for its coarser equivalent. This would imply that successive pulses of magma were intruded along the fault zones, after the volumetrically largest phases of the intrusion. Considering the narrow time interval of the dated intrusive units, and the lack of further evidence on the age of the “mine porphyry proper”, we tentatively estimate that it was emplaced 1889 ± 3 m.y. ago. If correct, it sets a minimum age for the VMS deposition, which is in agreement with the more loosely-defined minimum age constrained by the hanging-wall rhyolite.

5 Conclusions

The early-orogenic magmatism within the Kristineberg area occurred at ∼1.89 Ga when the Viterliden composite intrusion was emplaced during a period of ∼5 Ma. The intrusion was coeval with the emplacement of the earliest phases of the Jörn GI-type intrusions further east. The oldest phase of the Viterliden intrusion is a hornblende-tonalite (1892 ± 3 Ma) and the youngest is a quartz-plagioclase porphyritic tonalite (“mine porphyry”; 1889 ± 3 Ma). The emplacement of the latter was controlled by major faults. Volcanism in the Kristineberg area took place at 1.89–1.88 Ga and was contemporaneous with volcanism in the other parts of the Skellefte District. Furthermore, it defines the minimum age for the Kristineberg VMS deposit at ≥1.88 Ga. However, if the tentative correlation between the dated quartz-plagioclase porphyritic tonalite and the “mine porphyry proper” is correct, the minimum age is constrained even further, at 1889 ± 3 Ma. The age relationships between the volcanic and intrusive units within the Kristineberg area are compatible with the Viterliden intrusion being both the local basement for, and/or intruding into, the ore-hosting Skellefte Group volcanic rocks.

Acknowledgements. We thank Tobias Bauer for assistance in the field and for help in figure preparation. We warmly thank Martin Whitehouse, Lev Ilyinsky and Kerstin Lindén from the Nordsim laboratory for co-operation and help in the SIMS dating related issues. The Nordsim facility is financed and operated under an agreement between the research councils of Denmark, Norway and Sweden, the Geological Survey of Finland and the Swedish Museum of Natural History. This is Nordsim publication # XXX. This work is part of “VINNOVA 4D modelling of the Skellefte District” funded by VINNOVA, Boliden Mineral AB and Lundin Mining, and the “PROMINE” project partially funded by the European Commission under the 7th Framework Programme.

References

Allen, R. L., Weihed, P., and Svenson, S.-Å.: Setting of Zn-Cu-Au-Ag massive sulfide deposits in the evolution and facies architecture of a 1.9 Ga marine volcanic arc, Skellefte District, Sweden, Econ. Geol., 91, 1022–1053, 1996.

Årebäck, H., Barrett, T. J., Abrahamsson, S., and Fagerström, P.: The Palaeoproterozoic Kristineberg VMS deposit, Skellefte District, northern Sweden, part I: geology, Miner. Deposita, 40, 351–367, 2005.

Bauer, T.: Structural and Sedimentological Reconstruction of the Inverted Vargfors Basin – A base for 4D-modelling, Licentiate thesis, Luleå University of Technology, Sweden, 44 pp., 2010.

Bauer, T., Skyttä, P., Weihed, P., and Allen, R.: 3D-modelling of the Central Skellefte District, Sweden, Proceedings of the 10th biennial SGA meeting, Townsville, Australia, 394–396, 2009.

Bauer, T. E., Skyttä, P., Allen, R. L., and Weihed, P.: Syn-extensional faulting controlling structural inversion at the Svecokarelian Craton margin – Insights from the Palaeoproterozoic Vargfors basin, Skellefte mining district, Sweden, Precambrian Research, in review, 2011.

Bergman Weihed, J.: Palaeoproterozoic deformation zones in the Skellefte and the Arvidsjaur areas, northern Sweden, in: Economic Geology Research 1, edited by: Weihed, P., Sveriges Geologiska Undersökning, C 833, 46–68, 2001.

Billström, K. and Weihed., P.: Age and provenance of host rocks and ores of the Palaeoproterozoic Skellefte District, northern Sweden, Econ. Geol., 91, 1054–1072, 1996.

Bergström, U., Billström, K., and Sträng, T.: Age of the Kristineberg pluton, western Skellefte district, northern Sweden, in: Radiometric dating results 4, edited by: Bergman, S., Sveriges geologiska undersökning, C 831, 7–19, 1999.

Carranza, E. J. M. and Sadeghi, M.: Predictive mapping of prospectivity and quantitative estimation of undiscovered VMS deposits in Skellefte district (Sweden), Ore Geol. Rev., 38, 219–241, 2010.

Corfu, F., Hanchar, J. M., Hoskin, P. W. O., and Kinny, P.: Atlas of zircon textures, in: Zircon, Reviews in Mineralogy and Geochemistry, vol. 53, edited by: Hanchar, J. M. and Hoskin, P. W. O., Mineralogical Society of America, 468–500, 2003.

Dehghannejad, M., Juhlin, C., Malehmir, A., Skyttä, P., and Weihed, P.: Reflection seismic imaging of the upper crust in the Kristineberg mining area, northern Sweden, J. Appl.

Geophys., 71, 125–136, 2010.
Gaál, G.: Tectonic styles of early Proterozoic ore deposition in the Fennoscandian shield, Precambrian Res., 46, 83–114, 1990.
Hietanen, A.: Generation of potassium-poor magmas in the northern Sierra Nevada and the Svecofennian of Finland, J. Res. US Geol. Surv., 3, 631–645, 1975.
Kathol, B. and Weihed., P. (Eds.): Description of regional geological and geophysical maps of the Skellefte District and surrounding areas, Sveriges geologiska undersökning Ba 57, 197 pp., 2005.
Ludwig, K. R.: Isoplot/Ex. 3. A geochronological toolkit for Microsoft Excel, Berkeley Geochronology Center, Special Publication No. 4., 2003.
Lundström, I. and Antal, I.: Bedrock map 23 K Boliden, scale 1:50 000, Sveriges geologiska undersökning Ai, 110–113, 2000.
Lundström, I., Vaasjoki, M., Bergström, U., Antal, I., and Strandman, F.: Radiometric age determinations of plutonic rocks in the Boliden area: the Hobergsliden granite and the Stavaträsk diorite, in: Radiometric dating results 3, edited by: Lundqvist, T., Sveriges geologika undersökning, C 830, 20–30, 1997.
Malehmir, A., Tryggvason, A., Lickorish, H., and Weihed, P.: Regional structural profiles in the western part of the Palaeoproterozoic Skellefte ore district, northern Sweden, Precambrian Res., 159, 1–18, 2007.
Malehmir, A., Thunehed, H., and Tryggvason, A.: The Paleoproterozoic Kristineberg mining area, northern Sweden: Results from integrated 3D geophysical and geologic modelling, and implications for targeting ore deposits, Geophysics, 74, B9–B22, 2009.
Rutland, R. W. R, Kero, L., Nilsson, G., and Stølen, L. K.: Nature of a major tectonic discontinuity in the Svecofennian province of northern Sweden, Precambrian Res., 112, 211–237, 2001a.
Rutland, R. W. R., Skiöld, T., and Page, R. W.: Age of deformation episodes in the Palaeoproterozoic domain of northern Sweden, and evidence for a pre-1.9 Ga crustal layer, Precambrian Res., 112, 239–259, 2001b.
Skiöld, T.: Implications of new U-Pb zircon chronology to early Proterozoic crustal accretion in northern Sweden, Precambrian Res., 38, 147–164, 1988.
Skiöld, T. and Rutland, R. W. R.: Successive ~1.94 Ga plutonism and ~1.92 Ga deformation and metamorphism south of the Skellefte district, northern Sweden: Substantiation of the marginal basin accretion hypothesis of Svecofennian evolution, Precambrian Res., 148,

SED
3, 355–383, 2011

New zircon data supporting models of short-lived igneous activity at 1.89 Ga

P. Skyttä et al.

181–204, 2006.
Skiöld, T., Öhlander, B., Markkula, H., Widenfalk, L., and Claesson, L. Å.: Chronology of Proterozoic orogenic processes at the Archaean continental margin in northern Sweden, Precambrian Res., 64, 225–238, 1993.
Skyttä, P., Hermansson, T., and Bauer, T.: Three Dimensional Structure of the VMS-hosting Palaeoproterozoic Kristineberg Area, Northern Sweden. Proceedings of the 10th biennial SGA meeting, Townsville, Australia, 909–911, 2009.
Skyttä, P., Hermansson, T., Elming, S.-Å., and Bauer, T.: Magnetic fabrics as constraints on the kinematic history of a pre-tectonic granitoid intrusion, Kristineberg, northern Sweden, J. Struct. Geol., 32, 1125–1136, 2010.
Stacey, J. S. and Kramers, J. D.: Approximation of terrestrial lead isotope evolution by a two-stage model, Earth Palnet. Sc. Lett., 26, 207–221, 1975.
Weihed, P. and Schöberg, H.: Timing of porphyry type mineralizations in the Skellefte District, northern Sweden, GFF, 113, 289–294, 1991.
Weihed, P., Bergman, J., and Bergström, U.: Metallogeny and tectonic evolution of the early Proterozoic Skellefte District, northern Sweden, Precambrian Res., 58, 143–167, 1992.
Weihed, P., Billström, K., Persson, P.-O., and Bergman Weihed, J.: Relationship between 1.90–1.85 Ga accretionary processes and 1.82–1.80 Ga oblique subduction at the Karelian craton margin, Fennoscandian Shield, GFF, 124, 163–180, 2002.
Welin, E.: The depositional environment of the Svecofennian supracrustal sequence in Finland and Sweden, Precambrian Res., 35, 95–113, 1987.
Whitehouse, M. J. and Kamber, B. S.: Assigning dates to thin gneissic veins in high-grade metamorphic terranes: a cautionary tale from Akilia, southwest Greenland, J. Petrol., 46, 291–318, 2005.
Whitehouse, M. J., Kamber, B., and Moorbath, S.: Age significance of U-Th-Pb zircon data from early Archaean rocks of west Greenland – a reassessment based on combined ion-microprobe and imaging studies, Chem. Geol., 160, 201–224, 1999.
Wiedenbeck, M., Allé, P., Corfu, F., Griffin, W. L., Meier, M., Oberli, F., von Quadt, A., Roddick, J. C., and Spiegel, W.: Three natural zircon standards for U–Th-Pb, Lu-Hf, trace element and REE analysis, Geostandard. Newslett., 19, 1–23, 1995.
Wilson, M. R. Claesson, L.-Å., Sehlstedt, S., Smellie, J. A. T., Aftalion, M., Hamilton, P. J., and Fallick, A. E.: Jörn: An early Proterozoic intrusive complex in a volcanic arc environment, north Sweden, Precambrian Res., 36, 201–225, 1987.

SED
3, 355–383, 2011

Table 1. SIMS U-Th-Pb zircon data for the intrusive and volcanic rocks dated in this study. Data for point n3448-10a (sample I) is missing as it was planned and marked on the analysis plan, but finally not analyzed.

Sample[a]/ spot #	Analysed area: textural domain	Analysed area: location	[Pb] ppm	[U] ppm	Th[b]/U	$^{206}Pb/^{204}Pb$	$f^{206}Pb$[c] %	Ratios ± σ: $^{206}Pb/^{238}U$	± σ	Ratios ± σ: $^{207}Pb/^{206}Pb$	± σ	Age ± σ (Ma): $^{207}Pb/^{206}Pb$	± σ	Age ± σ (Ma): $^{206}Pb/^{238}U$	± σ	Disc. % 2σ lim.[d]
Sample I: Viterliden Hornblende tonalite (47.1-pmsk-09)																
n3448-01a	wk osc zon	cracked	190	439	0.53	65 130	0.03	0.3423	1.09	0.1154	0.27	1886	5	1898	18	
n3448-01b	wk osc zon		204	462	0.55	152 518	0.01	0.3480	1.21	0.1159	0.26	1894	5	1925	20	
n3448-02a	wk osc zon		52	122	0.40	206 770	< 0.01	0.3446	1.16	0.1162	0.50	1899	9	1909	19	
n3448-03a	wk osc zon		171	394	0.53	225 287	0.01	0.3418	1.15	0.1163	0.28	1899	5	1895	19	
n3448-04a	wk osc zon		163	384	0.47	47 375	0.04	0.3385	1.15	0.1157	0.29	1891	5	1880	19	
n3448-05a	wk osc zon		95	223	0.44	190 369	0.01	0.3416	1.10	0.1156	0.37	1890	7	1895	18	
n3448-06a	uz inner domain		200	467	0.51	68 717	0.03	0.3388	1.14	0.1155	0.26	1887	5	1881	19	
n3448-06b	uz outer domain	cracked	90	234	0.39	25 552	0.07	0.3115	1.10	0.1149	0.40	1878	7	1748	17	−5.1
n3448-07a	uz inner domain		273	598	0.65	218 045	0.01	0.3518	1.17	0.1159	0.23	1894	4	1943	20	0.4
n3448-08a	wk osc zon		163	374	0.48	155 575	0.01	0.3488	1.10	0.1154	0.31	1887	5	1929	18	
n3448-08b	wk osc zon		113	266	0.43	206 131	0.01	0.3427	1.16	0.1153	0.35	1885	6	1900	19	
n3448-09a	uz inner domain		163	384	0.44	249 095	0.01	0.3419	1.06	0.1154	0.33	1886	6	1896	18	
n3448-11a	wk osc zon		123	295	0.44	126 747	0.01	0.3354	1.06	0.1156	0.33	1889	6	1865	17	
n3448-12a	uz outer domain		200	457	0.54	282 209	0.01	0.3439	1.06	0.1160	0.26	1896	5	1906	18	
n3448-13a	uz sec domain	cracked	112	309	0.24	63 005	0.03	0.3032	1.08	0.1153	0.37	1884	7	1707	16	−8.1
Sample II: Viterliden plagioclase porphyritic tonalite (33.1-pmsk-08)																
n3450-01a	uz outer domain		49	121	0.27	100 267	0.02	0.3377	1.09	0.1163	0.50	1899	9	1875	18	
n3450-02a	uz outer domain		45	111	0.26	15 757	0.12	0.3361	1.11	0.1155	0.58	1887	10	1868	18	
n3450-02b	wk zon outer domain	cracked	49	128	0.24	58 176	0.03	0.3201	1.11	0.1148	0.56	1876	10	1790	17	−1.9
n3450-03a	uz outer domain		60	144	0.33	84 446	0.02	0.3412	1.11	0.1167	0.48	1907	9	1892	18	
n3450-03b	osc zon core		99	238	0.37	106 179	0.02	0.3410	1.09	0.1157	0.45	1891	8	1892	18	
n3450-04a	uz margin/osc core	crystal margin	55	140	0.30	50 501	0.04	0.3275	1.16	0.1167	0.88	1906	16	1826	18	−0.2
n3450-05a	wk zon outer domain		78	195	0.32	52 019	0.04	0.3312	1.12	0.1156	0.62	1889	11	1844	18	
n3450-06a	wk zon core		57	140	0.30	61 052	0.03	0.3378	1.13	0.1155	0.51	1888	9	1876	18	
n3450-07a	uz margin	crystal margin	56	148	0.24	20 809	0.09	0.3165	1.10	0.1143	0.50	1868	9	1773	17	−2.8
n3450-07b	uz		66	163	0.34	43 894	0.04	0.3340	1.07	0.1157	0.65	1891	12	1858	17	
n3450-08a	wk zon outer domain	cracked	43	228	0.09	4580	0.41	0.1599	1.10	0.1142	0.58	1868	10	956	10	−49.4
n3450-08b	wk zon outer domain	cracked, epoxy	96	747	0.12	467	4.00	0.1070	1.21	0.1067	1.12	1744	20	655	8	−59.7
n3450-09a	wk osc zon	cracked	51	141	0.26	3166	0.59	0.3021	1.14	0.1154	0.67	1886	12	1702	17	−7.4
n3450-09b	wk osc zon		54	126	0.35	41 408	0.05	0.3509	1.16	0.1153	0.64	1884	11	1939	19	
n3450-10a	wk zon bands		43	103	0.29	73 561	0.03	0.3459	1.09	0.1157	0.58	1891	10	1915	18	
n3450-11a	wk zon bands	inclusion	56	132	0.29	48 447	0.04	0.3537	1.13	0.1159	0.49	1895	9	1952	19	0.3
n3450-11b	wk zon bands		81	195	0.35	182 975	0.01	0.3428	1.06	0.1163	0.44	1900	8	1900	18	
n3450-12a	uz core		35	85	0.25	59 478	0.03	0.3440	1.09	0.1152	0.60	1882	11	1906	18	
n3450-13a	osc zon	cracked, epoxy	141	469	0.24	2223	0.84	0.2486	1.10	0.1131	0.54	1850	10	1431	14	−22.2
n3450-14a	uz core	cracked	51	146	0.22	52 445	0.04	0.2955	1.40	0.1152	0.49	1883	9	1669	21	−9.6
n3450-15a	wk osc zon	cracked, crystal margin	156	419	0.37	15 215	0.12	0.3013	1.08	0.1146	0.38	1874	7	1698	16	−8.1
n3450-16a	osc zon	crystal margin	269	800	0.37	37 558	0.05	0.2716	1.07	0.1122	0.28	1835	5	1549	15	−15.4
n3450-17a	wk osc zon	cracked	107	264	0.37	75 986	0.02	0.3318	1.06	0.1161	0.42	1897	7	1847	17	−0.2
n3450-18a	wk osc zon	cracked	191	471	0.48	44 536	0.04	0.3209	1.06	0.1160	0.34	1895	6	1794	17	−3.6
n3450-19a	wk osc zon		65	156	0.35	68 554	0.03	0.3391	1.07	0.1160	0.50	1896	9	1883	17	
n3450-20a	wk osc zon	inclusion	58	159	0.24	8383	0.22	0.3053	1.06	0.1140	0.56	1864	10	1717	16	−5.7
n3450-21a	osc zon	cracked, inclusion	163	458	0.39	34 098	0.05	0.2857	1.24	0.1154	0.32	1886	6	1620	18	−13.4
n3450-22a	wk osc zon	cracked	103	366	0.24	12 084	0.15	0.2312	1.32	0.1150	0.49	1880	9	1341	16	−28.9
n3450-23a	wk osc zon	cracked	63	182	0.30	6926	0.27	0.2835	1.12	0.1148	0.55	1877	10	1609	16	−13.0
n3450-24a	alt core	cracked	921	2180	0.50	77 295	0.02	0.3345	1.06	0.1158	0.14	1892	2	1860	17	
n3450-25a	wk osc zon		138	326	0.40	66 439	0.03	0.3439	1.08	0.1149	0.35	1878	6	1906	18	
n3450-26a	uz core	cracked	471	1197	0.49	69 280	0.03	0.3102	1.12	0.1150	0.25	1880	5	1742	17	−6.0

SED
3, 355–383, 2011

Table 1. Continued.

Sample[a]/ spot #	Analysed area: textural domain	Analysed area: location	[Pb] ppm	[U] ppm	Th[b]/U	^{206}Pb/^{204}Pb	f^{206}Pb[c] %	Ratios ± σ: ^{206}Pb/^{238}U	±σ	Ratios ± σ: ^{207}Pb/^{206}Pb	±σ	Age ± σ (Ma): ^{207}Pb/^{206}Pb	±σ	Age ± σ (Ma): ^{206}Pb/^{238}U	±σ	Disc. % 2σ lim.[d]
Sample III: Viterliden quartz-plagioclase porphyritic tonalite (coarse "mine-porphyry"; 29.1-pmsk-08)																
n3449-01a	uz	cracked	127	343	0.21	6818	0.27	0.3147	1.11	0.1153	0.64	1884	11	1764	17	−3.7
n3449-02a	osc zon		237	573	0.27	65 615	0.03	0.3473	1.11	0.1155	0.23	1888	4	1922	18	
n3449-03a	osc zon		164	406	0.23	87 815	0.02	0.3415	1.11	0.1151	0.28	1882	5	1894	18	
n3449-04a	osc zon		159	397	0.22	33 500	0.06	0.3396	1.10	0.1160	0.30	1895	5	1885	18	
n3449-05a	uz core	cracked	237	580	0.63	4554	0.41	0.3116	1.15	0.1151	0.36	1882	6	1748	18	−5.4
n3449-06a	osc zon	cracked	287	762	0.32	9097	0.21	0.3095	1.45	0.1159	0.30	1894	5	1738	22	−6.4
n3449-07a	osc zon	epoxy	160	528	0.16	2936	0.64	0.2584	1.78	0.1138	0.47	1860	9	1481	24	−19.3
n3449-08a	osc zon	margin	303	831	0.31	7942	0.24	0.2998	1.11	0.1140	0.26	1865	5	1690	16	−8.3
n3449-08b	osc zon		253	617	0.29	62 164	0.03	0.3421	1.07	0.1154	0.26	1886	5	1897	18	
n3449-09a	wk osc zon		141	356	0.19	69 422	0.03	0.3380	1.10	0.1158	0.30	1892	5	1877	18	
n3449-10a	osc zon		239	594	0.28	17 957	0.10	0.3355	1.06	0.1156	0.35	1890	6	1865	17	
n3449-11a	alt osc zon	cracked	206	1019	0.12	1650	1.13	0.1714	1.35	0.1160	0.75	1895	13	1020	13	−46.0
n3449-12a	osc zon	cracked	216	556	0.25	12 574	0.15	0.3263	1.08	0.1155	0.29	1887	5	1820	17	−1.6
n3449-13a	osc zon	cracked	293	775	0.25	10 292	0.18	0.3177	1.07	0.1151	0.25	1882	5	1778	17	−4.0
n3449-14a	osc zon	epoxy	239	644	0.17	3173	0.59	0.3175	1.10	0.1154	0.40	1886	7	1778	17	−3.8
n3449-15a	uz	cracked	137	402	0.15	5806	0.32	0.2923	1.06	0.1151	0.44	1882	8	1653	15	−11.1
n3449-16a	osc zon	epoxy, cracked	179	639	0.13	2513	0.74	0.2392	1.32	0.1144	0.55	1871	10	1383	16	−25.8
n3449-17a	wk osc zon	cracked	201	535	0.23	79 531	0.02	0.3157	1.06	0.1150	0.27	1879	5	1769	16	−4.4
n3449-18a	osc zon	slightly cracked	235	595	0.22	10 743	0.17	0.3335	1.06	0.1160	0.34	1896	6	1856	17	
n3449-19a	osc zon	margin	268	661	0.36	12 333	0.15	0.3327	1.06	0.1152	0.32	1883	6	1851	17	
n3449-20a	wk osc zon		197	491	0.20	259 299	0.01	0.3423	1.07	0.1161	0.27	1897	5	1898	18	
n3449-21a	alt osc zon	cracked	240	626	0.25	4684	0.40	0.3216	1.66	0.1149	0.31	1879	6	1797	26	−1.5
n3449-22a	osc zon	cracked	204	545	0.23	12 079	0.15	0.3150	1.10	0.1160	0.28	1896	5	1765	17	−5.5
n3449-23a	osc zon	inclusion	254	875	0.20	3506	0.53	0.2432	1.14	0.1155	0.31	1888	5	1403	14	−26.4
n3449-24a	osc zon	slightly cracked	182	470	0.22	27 240	0.07	0.3283	1.06	0.1154	0.37	1886	7	1830	17	−0.7
n3449-25a	osc zon	inclusion, cracked	268	765	0.25	4358	0.43	0.2917	1.12	0.1157	0.29	1890	5	1650	16	−12.1
n3449-26a	osc zon	cracked	160	406	0.25	7382	0.25	0.3300	1.06	0.1162	0.38	1898	7	1839	17	−1.0
Sample IV: Kristineberg hanging wall Rhyolite (60.1-pmsk-09)																
n3447-01a	uz core	cracked	149	338	0.43	33 819	0.06	0.3570	1.19	0.1158	0.60	1893	11	1968	20	0.8
n3447-02a	uz eu tip		69	163	0.29	8237	0.23	0.3564	1.10	0.1147	0.67	1875	12	1965	19	1.7
n3447-03a	uz outer	margin	29	91	0.17	1779	1.05	0.2704	1.11	0.1112	1.34	1820	24	1543	15	−10.7
n3447-04a	uz eu tip	margin	98	284	0.29	3271	0.57	0.2838	1.32	0.1127	0.71	1844	13	1611	19	−10.3
n3447-04b	uz core/tip	cracked	136	325	0.40	13 230	0.14	0.3414	1.11	0.1151	0.43	1881	8	1894	18	
n3447-05a	uz inner	cracked	111	484	0.21	33 918	0.06	0.1868	1.09	0.1154	0.45	1885	8	1104	11	−42.6
n3447-05b	uz outer	epoxy	41	164	0.12	1129	1.66	0.2181	1.26	0.1055	2.15	1723	39	1272	15	−18.5
n3447-06a	eu wk zon inner domain	inclusion, cracked	119	266	0.39	34 719	0.05	0.3665	1.12	0.1153	0.45	1884	8	2013	19	4.7
n3447-07a	eu uz		122	278	0.36	24 422	0.08	0.3627	1.11	0.1155	0.45	1887	8	1995	19	3.5
n3447-08a	uz inner domain	cracked	137	315	0.42	23 710	0.08	0.3528	1.11	0.1149	0.52	1878	9	1948	19	1.0
n3447-09a	eu wk zon inner domain		35	83	0.24	10 833	0.17	0.3595	1.19	0.1134	0.86	1854	15	1980	20	3.1
n3447-09b	eu wk zon inner domain		72	165	0.30	29 061	0.06	0.3633	1.11	0.1149	0.63	1879	11	1998	19	3.6
n3447-10a	eu wk zon tip	epoxy	49	126	0.23	1183	1.58	0.3340	1.11	0.1067	1.48	1744	27	1858	18	
n3447-10b	eu wk zon inner domain		77	182	0.30	21 703	0.09	0.3521	1.10	0.1144	0.61	1870	11	1945	19	1.0
n3447-11a	eu wk zon inner domain		49	116	0.26	12 974	0.14	0.3585	1.13	0.1151	0.86	1882	15	1975	19	1.1
n3447-12a	eu uz	cracked	94	220	0.38	14 732	0.13	0.3470	1.11	0.1161	0.59	1897	11	1920	18	
n3447-13a	uz fragment		100	236	0.32	5761	0.32	0.3527	1.10	0.1147	0.71	1875	13	1948	18	0.5
n3447-14a	eu uz fragm	cracked	58	143	0.36	7551	0.25	0.3292	1.10	0.1150	0.76	1879	14	1834	18	
n3447-15a	uz	margin	45	170	0.18	10 873	0.17	0.2240	1.11	0.1143	1.14	1869	20	1303	13	−28.0
n3447-16a	uz	margin	37	92	0.20	3120	0.60	0.3466	1.10	0.1115	1.15	1824	21	1919	18	0.0
n3447-17a	uz tip	inclusion, margin	83	204	0.37	3260	0.57	0.3337	1.12	0.1147	0.67	1875	12	1856	18	
n3447-18a	uz		101	231	0.42	12 187	0.15	0.3561	1.11	0.1138	0.64	1862	12	1964	19	2.5
n3447-19a	uz	margin	74	189	0.31	8919	0.21	0.3260	1.17	0.1153	0.73	1885	13	1819	19	
n3447-20a	uz	epoxy, cracked	155	494	0.34	899	2.08	0.2569	1.34	0.1040	2.19	1697	40	1474	18	−4.0

SED
3, 355–383, 2011

Table 1. Continued.

Sample[a]/ spot #	Analysed area: textural domain	Analysed area: location	[Pb] ppm	[U] ppm	$\frac{Th}{U}$[b]	$\frac{^{206}Pb}{^{204}Pb}$	$f^{206}Pb$[c] %	Ratios ± σ: $\frac{^{206}Pb}{^{238}U}$	± σ	Ratios ± σ: $\frac{^{207}Pb}{^{206}Pb}$	± σ	Age ± σ (Ma): $\frac{^{207}Pb}{^{206}Pb}$	± σ	Age ± σ (Ma): $\frac{^{206}Pb}{^{238}U}$	± σ	Disc. % 2σ lim.[d]
n3447-21a	uz	cracked	116	277	0.36	24 060	0.08	0.3459	1.09	0.1140	0.53	1864	10	1915	18	
n3447-22a	uz	cracked	48	119	0.22	5157	0.36	0.3443	1.21	0.1144	0.88	1870	16	1907	20	
n3447-23a	uz inner domain	cracked	65	156	0.28	5497	0.34	0.3473	1.09	0.1154	0.81	1886	15	1922	18	
n3447-24a	*uz inner domain*	*inclusion, cracked*	*111*	*344*	*0.36*	*8670*	*0.22*	*0.2580*	*1.46*	*0.1144*	*0.52*	*1871*	*9*	*1480*	*19*	*−20.1*
n3447-25a	*uz outer domain*	*cracked*	*122*	*273*	*0.50*	*7691*	*0.24*	*0.3596*	*1.14*	*0.1146*	*0.55*	*1874*	*10*	*1980*	*19*	*3.1*
n3447-26a	*wk zon outer domain*	*margin*	*53*	*390*	*0.11*	*6713*	*0.28*	*0.1136*	*2.88*	*0.1138*	*0.75*	*1861*	*13*	*694*	*19*	*−61.8*
n3447-27a	*eu uz inner domain*	*cracked*	*139*	*316*	*0.41*	*19 640*	*0.10*	*0.3590*	*1.25*	*0.1149*	*0.44*	*1878*	*8*	*1977*	*21*	*2.8*
n3447-28a	*uz inner domain*	*cracked*	*46*	*110*	*0.27*	*3302*	*0.57*	*0.3553*	*1.14*	*0.1133*	*0.84*	*1853*	*15*	*1960*	*19*	*2.0*
n3447-29a	uz	epoxy	72	176	0.22	46 998	0.04	0.3451	1.10	0.1156	0.92	1890	16	1911	18	
n3447-30a	uz inner domain	inclusion, cracked	97	228	0.40	13 042	0.14	0.3456	1.15	0.1150	0.57	1880	10	1914	19	
n3447-31a	*eu uz*	*margin*	*52*	*204*	*0.19*	*1064*	*1.76*	*0.2210*	*####*	*0.0936*	*5.18*	*1501*	*95*	*1287*	*138*	
n3447-32a	*wk zon inner domain*	*margin*	*113*	*267*	*0.29*	*35 983*	*0.05*	*0.3542*	*1.10*	*0.1162*	*0.54*	*1898*	*10*	*1955*	*19*	*0.1*
n3447-32b	wk zon inner domain		121	299	0.23	54 511	0.03	0.3409	1.09	0.1161	0.47	1897	8	1891	18	

[a] Data used for age calculation shown with normal letters; data in italics have been excluded from age calculation.
[b] Th/U ratios calculated from $^{208}Pb/^{206}Pb$ ratios corrected for common Pb.
[c] % of common ^{206}Pb in measured ^{206}Pb, estimated from ^{204}Pb assuming a present day Stacey and Kramers (1975) model.
[d] Degree of discordance; positive numbers are reverse discordant. Blanks indicate that analysis is concordant within 2σ error. Abbreviations: zon = zonation, osc = oscillatory, wk = weak, uz = unzoned, eu = euhedral crystal, alt = altered.

SED
3, 355–383, 2011

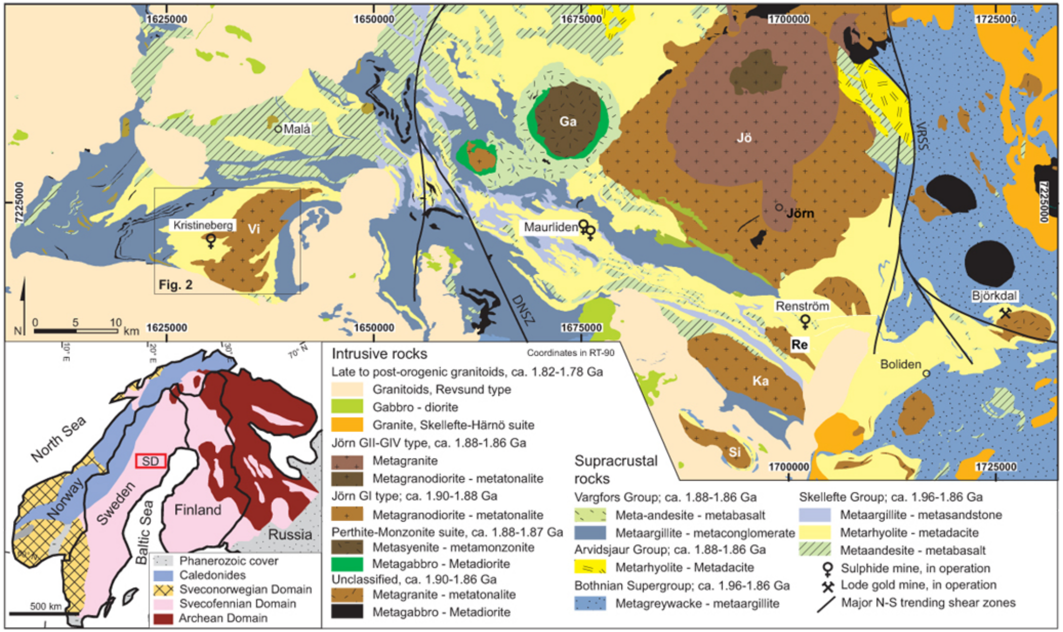

Fig. 1. Inset: geological overview of the Fennoscandian Shield. SD = Skellefte District. Main map: DNSZ = Deppis-Näsliden shear zone; VRSS = Vidsel-Röjnöret shear system; Intrusions: Ga = Gallejaur, Jö = Jörn, Ka = Karsträsk, Re = Rengård, Si = Sikträsk, Vi = Viterliden. Geology after the Geological Survey of Sweden, and Bergman Weihed (2001).

SED
3, 355–383, 2011

New zircon data supporting models of short-lived igneous activity at 1.89 Ga

P. Skyttä et al.

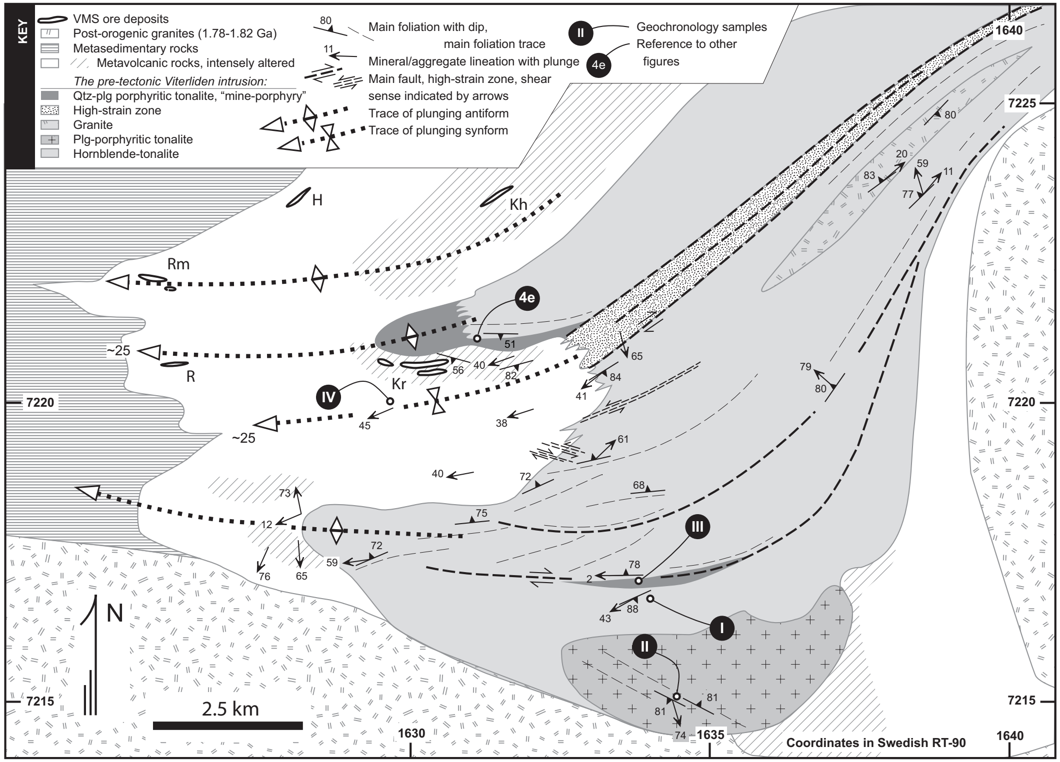

Fig. 2. Geological map of the Viterliden intrusion with locations for the geochronology samples. Modified after Skyttä et al. (2010). Ore deposits: Kr = Kristineberg, Kh = Kimheden, H = Hornträsk, Rm = Rävlidmyran, R = Rävliden.

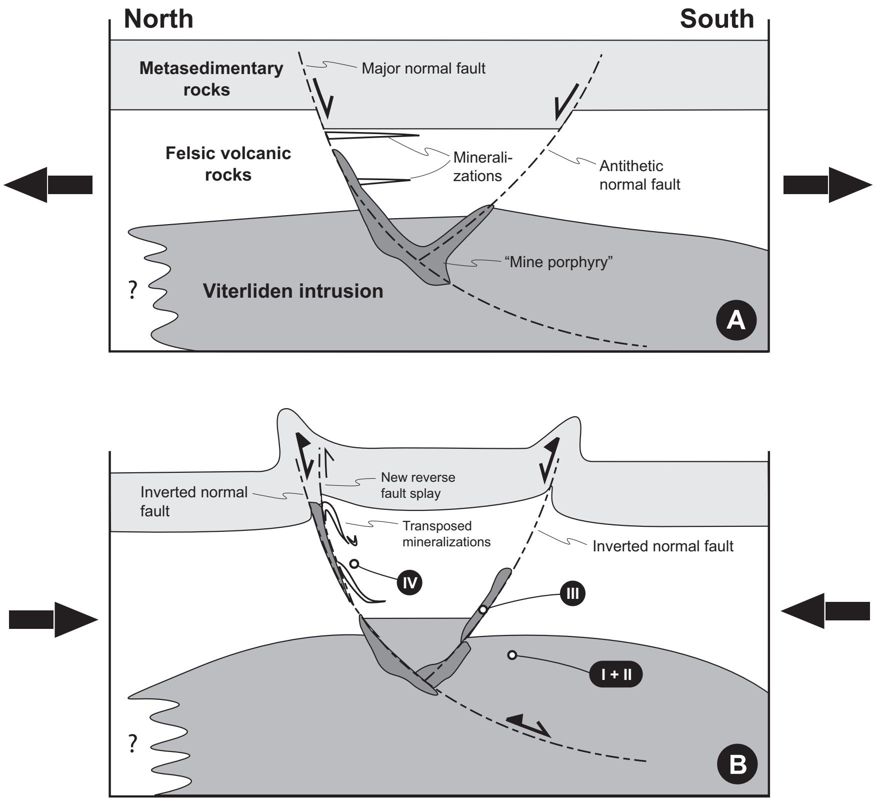

Fig. 3. Schematic stratigraphic profile across the Kristineberg area including the location of the geochronology samples. Upper mineralized horizon = Hornträsk-Rävlidsmyran-Rävliden, lower mineralized horizon = Kristineberg-Kimheden. Metasedimentary and metavolcanic rocks belong to the Vargfors and the Skellefte Groups, respectively. **(A)** Syn-extensional volcanism, mineralization, sedimentation ± intrusive activity at ∼1.89–1.87 Ga. **(B)** Subsequent crustal shortening leading to basin inversion and related transposition of the mineralized horizons.

SED
3, 355–383, 2011

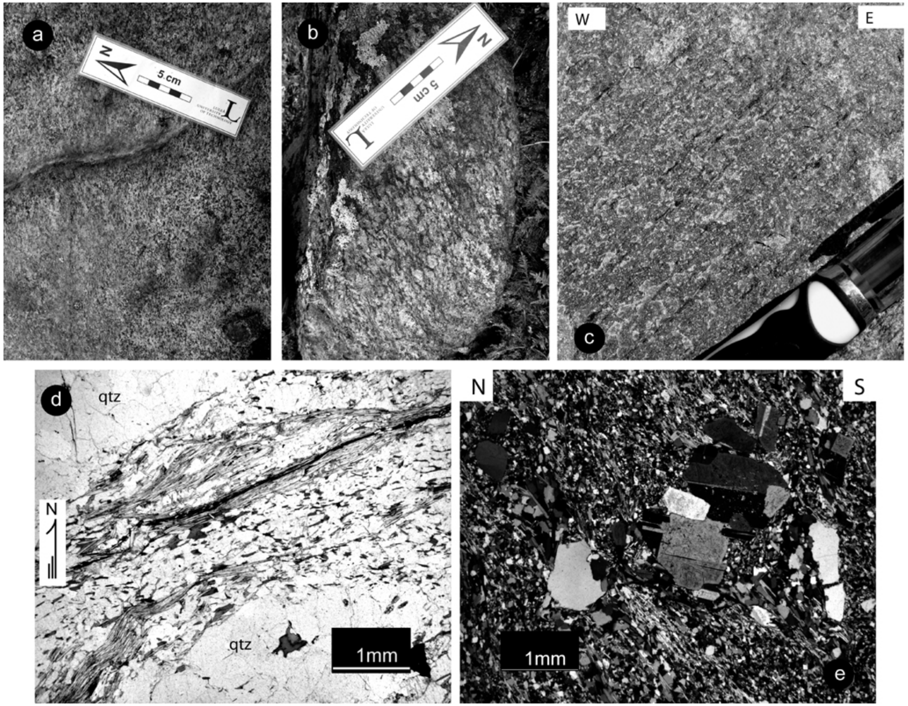

Fig. 4. Field and microphotographs of the dated rock units. See Fig. 2 for locations. **(a)** Viterliden hornblende-tonalite; geochronology sample I, **(b)** Viterliden plagioclase porphyritic tonalite; geochronology sample II, **(c)** Kristineberg hanging-wall rhyolite; geochronology sample IV; vertical section, width of view ~5 cm, **(d)** Viterliden quartz-plagioclase porphyritic tonalite (coarse "mine porphyry"); geochronology sample III and **(e)** quartz-plagioclase porphyritic tonalite ("mine porphyry").

SED
3, 355–383, 2011

New zircon data supporting models of short-lived igneous activity at 1.89 Ga

P. Skyttä et al.

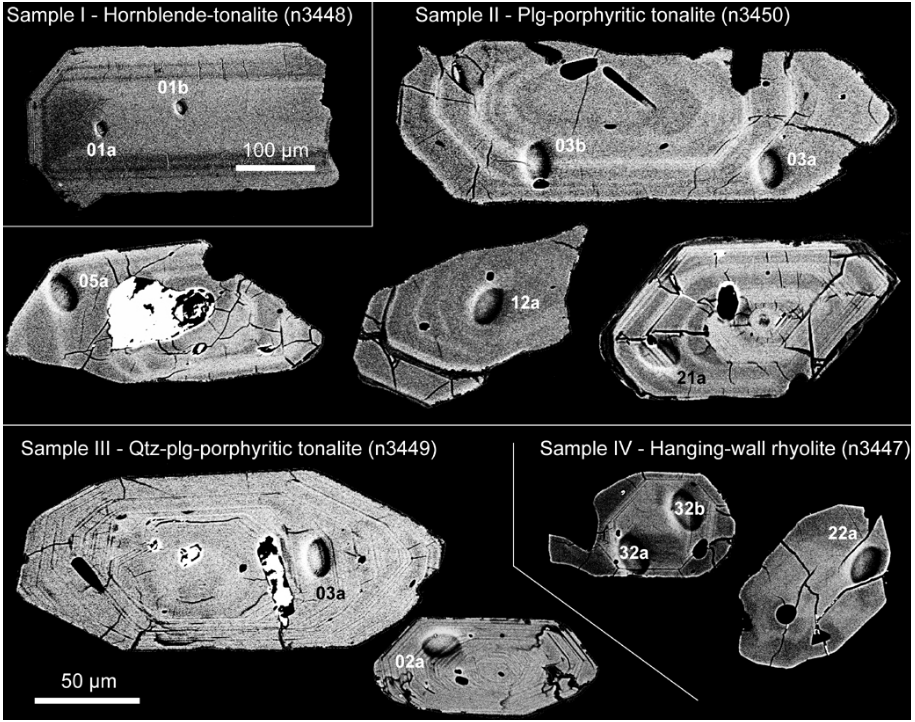

Fig. 5. BSE images for selected ion microprobe-dated zircons. Site of analyses are indicated by analyze number, see also Table 1. Note the different scale in n3448-01ab. Qtz = quartz, plg = plagioclase.

SED
3, 355–383, 2011

SED
3, 355–383, 2011

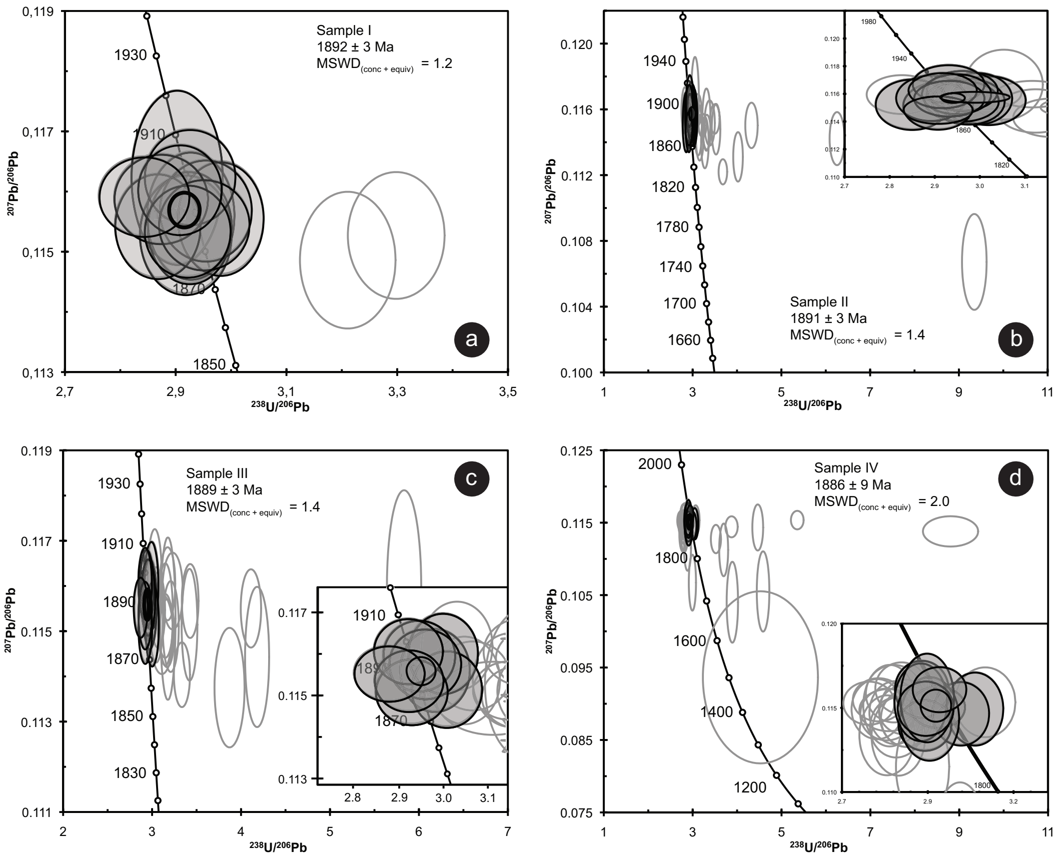

Fig. 6. Concordia diagrams for the dated rock units. **(a)** Sample I: Viterliden hornblende-tonalite (47.1-pmsk-09), **(b)** Sample II: Viterliden plagioclase porphyritic tonalite (33.1-pmsk-08), **(c)** Sample III: Viterliden quartz-plagioclase porphyritic tonalite (coarse "mine porphyry"; 29.1-pmsk-08), **(d)** Sample IV: Kristineberg hanging-wall rhyolite (60.1-pmsk-09).